Optically detected low-field ESR in the metastable state of Tm^{2+}:SrF_2. I. ESR signals and cross relaxation

T. Kohmoto, Y. Fukuda, and T. Hashi
Department of Physics, Faculty of Science, Kyoto University, Kyoto 606, Japan
(Received 9 June 1986)

ESR signals of Tm^{2+}:SrF_2 are observed in the ground ($^2F_{7/2}$,$E_{5/2}$) and metastable ($^2F_{5/2}$,$E_{5/2}$) states in low magnetic fields (0—300 Oe) at liquid-helium temperatures. We achieved a very high detection sensitivity ($\sim 10^9$ spins in the ground state) using optical means; the population differences are created by circular dichroism and spin memory, and the change of the Faraday rotation is detected by a polarimeter. Several interesting phenomena were observed. The signals in the ground and metastable states appeared with opposite polarities. The preferential pumping from the metastable state was examined by a double pumping experiment. We also measured the Faraday rotation between 4000 and 7000 Å. The experimental results suggest that the magnetization in the metastable state created by the preferential pumping from the ground state followed by the spin memory is in the opposite direction to that in the ground state. Anomalous behavior of the metastable-state signals was observed both in frequency and time domains. These are explained as an effect of the metastable-state—ground-state cross relaxation enhanced by the ground-state—ground-state cross relaxation.

I. INTRODUCTION

Impurity-ion-containing solids with the divalent thulium ion Tm^{2+} in alkaline-earth fluoride hosts, CaF_2, SrF_2, and BaF_2, have attractive properties. Several interesting experiments on spin-orientation memory,[1] enhancement of nuclear polarization by optical pumping,[2] and spin-phonon interactions[3] have been performed on Tm^{2+} in CaF_2. The optical[4–10] and magnetic[11–20] properties of Tm^{2+} in CaF_2, SrF_2, and BaF_2 have been extensively studied. The ground-state configuration of the Tm^{2+} ion is best pictured as a single hole in the filled $4f$ shell. This ion has strong absorption bands in the visible region with large paramagnetic circular dichroism in these host crystals.[9,21] The g factors and hyperfine constants were measured both in the ground[11,22] ($^2F_{7/2}$,$E_{5/2}$) and metastable[13,16] ($^2F_{5/2}$,$E_{5/2}$) states by paramagnetic resonance absorption. Superhyperfine interactions with fluorine nuclei were also studied by using the electron-nuclear double resonance technique.[12,16,20] Recently we observed ESR free-induction decay in the nanosecond time region by purely optical means in Tm^{2+}:SrF_2.[23]

In this paper we report on the observation of low-field ESR in the metastable state as well as in the ground state of Tm^{2+} in SrF_2. We achieved a very high detection sensitivity ($\sim 10^9$ spins) by using optical pumping and monitoring with cw lasers. The optical pumping with circularly polarized light creates population differences in the ground state through preferential depopulation due to the circular dichroism. It also creates population differences in the metastable state through the preferential pumping to the band and the spin memory from the band to the metastable state. Faraday rotation due to these population differences are monitored by a polarimeter. This method proves to be very sensitive, and convenient especially for a low-field ESR in the ground and optically excited states. Optical pumping creates a large population difference even in low magnetic fields where the thermal-equilibrium population difference is small. The detection making use of Faraday rotation substantially improves the sensitivity through the scaling up of the detection from the microwave or rf to the optical region.

Several interesting features of the low-field ESR signals were observed. We found that the ground and metastable state signals appeared with opposite polarities. The effect of preferential pumping from the metastable state was demonstrated by a double pumping experiment. It was found that the preferential pumping from the metastable state creates magnetization in that state in the same direction as that in the ground state. We deduced the signs of the population differences responsible for the signals using the result of the double pumping experiment or the measurement of Faraday rotation at a high magnetic field. Experimental results suggest that, for the single pumping, the magnetization created in the metastable state by the preferential pumping from the ground state followed by the spin memory effect is in the opposite direction to the magnetization in the ground state for the optical pumping at 5800 Å. The competition of the effects of spin memory and the preferential pumping from the metastable state was also observed.

We found anomalous behavior of the metastable-state signals when the frequency of the rf field was changed from 135 to 155 MHz. The effect became significant at 167 Oe, which is in the middle of the two crossing fields, 161.2 and 171.5 Oe; the former is for the metastable-state—ground-state cross relaxation and the latter for the ground-state—ground-state cross relaxation. These behaviors are explained as a result of the metastable-state—ground-state cross relaxation enhanced by the ground-state—ground-state cross relaxation.

Experimental results and a qualitative interpretation are

presented in this paper. The signs of the g factor and the hyperfine constant are determined in the following paper (part II).[24] The detailed analysis of the spin memory effect is planned to be given in a forthcoming paper (part III).[25]

II. ENERGY LEVELS OF Tm^{2+}:SrF_2

The divalent thulium ion with a $4f^{13}$ configuration has two spin-orbit states $^2F_{5/2}$ and $^2F_{7/2}$ with the latter lower. A cubic field (O_h) splits these states as shown in Fig. 1.[4,16] Electric dipole transitions from the ground state ($^2F_{7/2}$,$E_{5/2}$) to the $4f^{12}5d$ configuration form a broad absorption band starting at about 7000 Å. These transitions show magnetic circular dichroism[21] (MCD) and Faraday rotation (FR). The excited state ($^2F_{5/2}$,$E_{5/2}$) is metastable and the fluorescence lifetime is about 13 msec at 1.6 K (in our case). Transitions from the metastable state to the band also exhibit MCD and FR, although no detailed measurement has been made.

The ground and metastable states are Kramers doublets. They have hyperfine splittings due to the interaction with Tm nuclei ($I=\frac{1}{2}$) and the spin Hamiltonians in the magnetic field $\mathbf{H}$ (neglecting the nuclear Zeeman interaction) can be written as

$$\mathcal{H}=g\mu_B\mathbf{S}\cdot\mathbf{H}+A\mathbf{S}\cdot\mathbf{I}\ , \tag{1}$$

with effective electron spin $S=\frac{1}{2}$ and hyperfine constant A. Energy eigenvalues are of the same form in the ground and metastable states and are obtained from Hamiltonian (1) as

$$\begin{aligned}
E_1&=-\tfrac{1}{2}g\mu_BH+\tfrac{1}{4}A\ ,\\
E_2&=-\tfrac{1}{2}g\mu_BH[1+(A/g\mu_BH)^2]^{1/2}-\tfrac{1}{4}A\ ,\\
E_3&=\tfrac{1}{2}g\mu_BH+\tfrac{1}{4}A\ ,\\
E_4&=\tfrac{1}{2}g\mu_BH[1+(A/g\mu_BH)^2]^{1/2}-\tfrac{1}{4}A\ .
\end{aligned} \tag{2}$$

The eigenfunctions are also of the same form in the ground and metastable states and given by

$$\begin{aligned}
|1\rangle&=|--\rangle\ ,\\
|2\rangle&=a\,|-+\rangle+b\,|+-\rangle\ ,\\
|3\rangle&=|++\rangle\ ,\\
|4\rangle&=a\,|+-\rangle-b\,|-+\rangle\ ,
\end{aligned} \tag{3}$$

where $a=\cos(\theta/2)$, $b=\sin(\theta/2)$, $\theta=\tan^{-1}|A/g\mu_BH|$, and $|\pm\pm\rangle$ represents $|S_z=\pm\frac{1}{2},I_z=\pm\frac{1}{2}\rangle$. In the following we use asterisk (*) for the expressions in the metastable state to distinguish them from those in the ground state. The g factors and the hyperfine constants of the ground and metastable states are isotropic and known to be $|g|=3.445$ and $|A|=1102.5$ MHz (Ref. 22) for the ground state and $|g^*|=1.449$ and $|A^*|=1163$ MHz (Ref. 16) for the metastable state. The energy-level diagrams in low magnetic fields are shown in the insets of Fig. 1. The signs of g and A used in Fig. 1 ($g>0, A<0$ and $g^*<0, A^*>0$) are determined as described in paper II.[24] Since the signs of g and A are different in the ground and metastable states, the patterns of the energy levels are different.

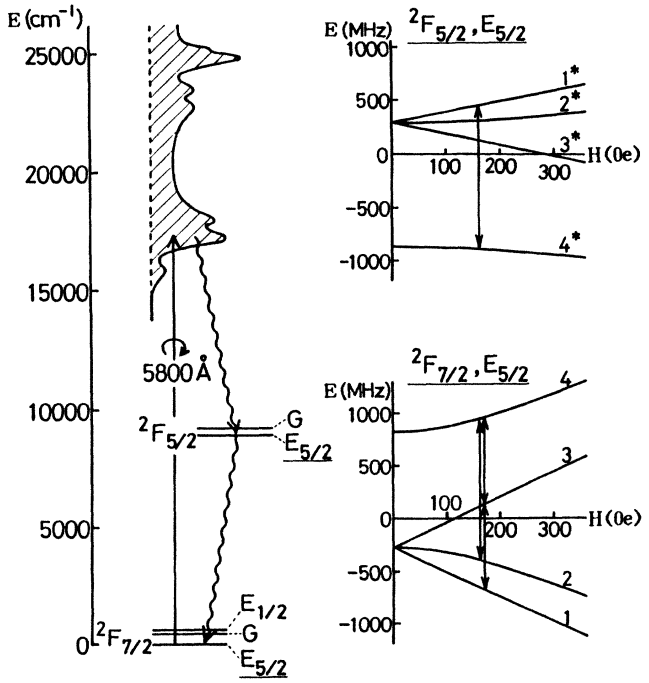

FIG. 1. Energy levels of Tm^{2+}:SrF_2.

III. EXPERIMENTAL PROCEDURE

The setup for the ESR experiment is schematically shown in Fig. 2(a). The pump and probe lights are provided by an Ar-laser-pumped dye laser and a He-Ne laser (6328 Å, 1 mW), respectively. The pump (circularly polarized) and probe (linearly polarized) beams are nearly collinear (parallel to the [111] axis) and focused on the sample (0.02 at. % Tm^{2+}, 2 mm in thickness) immersed in liquid helium (1.6 K). The waist sizes of the beams at the focus are about 100 μm. The wavelength of the pump beam is ~5750–5950 Å, and the maximum power in front of the cryostat is about 30 mW. A static magnetic field up to 300 Oe is applied parallel to the laser beams. Population differences in the magnetic sublevels are created by the pump beam. An rf field of 120–220 MHz, which is turned on and off at 26 Hz, is applied perpendicular to the static magnetic field. When the rf field is resonant on one of the transitions, the population difference, and therefore the FR, is changed. This change (ESR signal) is detected by a polarimeter and recorded on a chart recorder after lock-in detection and amplification.

The construction of the polarimeter[26,27] is shown in Fig. 2(b). A linearly polarized probe beam is split by a Glan prism and incident on the two photodiodes whose photocurrents are subtracted at a resistor. The Glan prism and the photodiodes are compactly and solidly assembled and can be rotated together. When the Glan

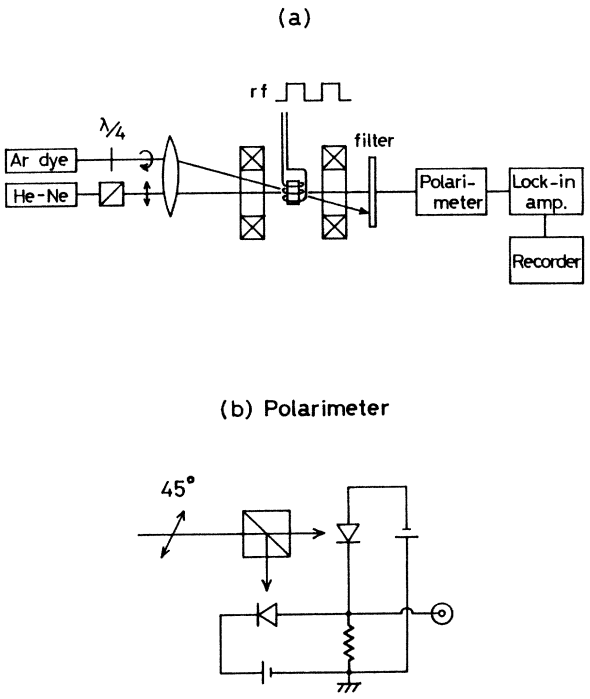

FIG. 2. (a) Setup for the ESR experiment and (b) construction of the polarimeter.

prism is mounted at an angle of 45° to the plane of polarization of the probe beam, the two photocurrents cancel. If the plane of polarization of the probe beam rotates, the two currents do not cancel and the voltage appears at the resistor.

The output P of the polarimeter can be represented as

$$P=K[E_0\sin(\pi/4+\theta)]^2-K[E_0\cos(\pi/4+\theta)]^2$$
$$=KE_0^2\sin(2\theta)$$
$$\simeq 2KE_0^2\theta \quad (\theta \ll 1)\,, \tag{4}$$

where θ is the FR angle, E_0 is the amplitude of the probe beam, and K is a constant. The ESR signals are detected through the change of the output P. The output linearly responds to the FR angle, when the angle θ is small. From Eq. (4) we obtain

$$\theta \simeq P/(2KE_0^2)$$
$$=P/(4P_0)\,, \tag{5}$$

where $P_0=KE_0^2/2$. At zero magnetic field ($\theta=0$), the output P given by Eq. (4) becomes zero, but if one of the photodiodes in the polarimeter is blocked the polarimeter output gives the value of P_0.

The polarimeter has a very high sensitivity and has the following advantages over cross polarizers. (1) It is not affected by disturbance of the polarization of the probe beam at the windows of the cryostat, etc., as long as the disturbance is static. (2) The output linearly responds to the population difference when the angle of FR is small. (3) The fluctuations of laser intensity are compensated by the balancing circuit. (4) It is very compact and easy to handle. The drawback is that it is sensitive to the position of the probe beam at the detector.

IV. EXPERIMENTAL RESULTS AND DISCUSSIONS

A. Typical ESR signals

Typical ESR signals obtained at the frequencies 120, 160, and 200 MHz under the pumping with σ^- light (5800 Å, 30 mW) are shown in Fig. 3. In our low-frequency experiment, ground-state ESR signals for the transitions 2-3 and 1-2, and metastable ones for 2*-3* and 1*-2* (Fig. 1) are expected. The upward two peaks in 3(a) and 3(b), which overlap in 3(c), are ground-state signals for the transitions 2-3 and 1-2. The small peak at the left is due to the forbidden transition 1-3. This peak became comparable to the other peaks when the intensity of the rf field was increased. The downward signals in higher magnetic fields are those in the metastable state corresponding to the transitions 2*-3* and 1*-2*. For these signals the amplifier gain is increased by 20. All signals appear at the positions expected from known values of $|g|$ and $|A|$ within experimental errors.

The ESR signals were detected through the change of FR of the probe beam. The changes of FR angles for the ground- and metastable-state signals obtained from Eq. (5) were ~ 2 and ~ 0.1 mrad, respectively. The number of spins contributing to the ground-state signal can be estimated to be 10^{12} by using the values of the optical

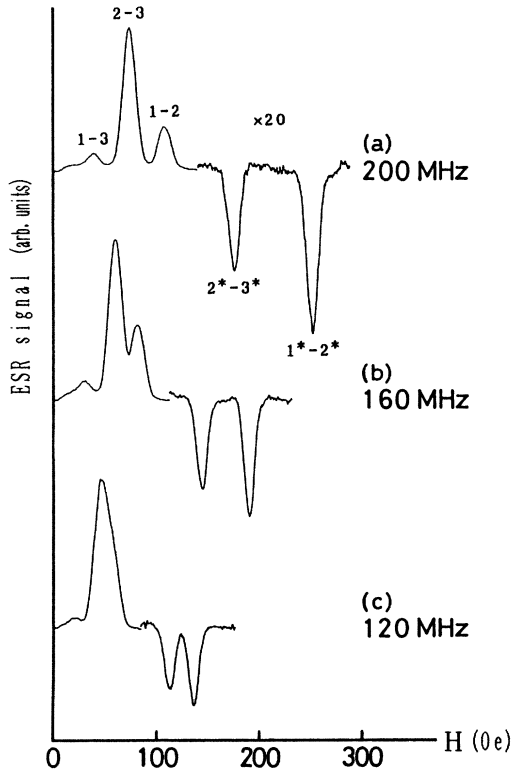

FIG. 3. ESR signals obtained at the frequencies (a) 120 MHz, (b) 160 MHz, and (c) 200 MHz under the pumping with σ^- light (5800 Å, 30 mW). For the metastable-state signals (on the right-hand sides) the amplifier gain is increased by 20.

pumping time (3 msec), the circular dichroism [~ 0.2 at 5800 Å, Fig. 5(b)], the density of Tm^{2+} ion [4×10^{18} ions/cm^3 for 0.02 at.% (Ref. 14)], and the pumped volume [$\sim(100\ \mu m)^2\times 2$ mm]. A few percent of the Tm ions in the pumped volume contributes to the ground-state signal. The derivation of the number of spins contributing to the metastable-state signal is difficult, since we do not have enough information about the metastable state. The minimum detectable FR angle is 2 μrad and it corresponds to 10^9 spins in the ground state.

The ground-state signals were detected even without dye-laser pumping, but the optical pumping enhanced the signals by a factor of $\sim 10^2$. The metastable-state signals were detected only in the presence of the optical pumping.

The linewidths of the ground- and metastable-state signals are 13 and 11 Oe, respectively, and can be attributed to the superhyperfine interaction between the Tm^{2+} ion and neighboring fluorine nuclei.[16,20,23]

Intensities I_{12} and I_{23} of the ground-state signals for the transitions 1-2 and 2-3 should be proportional to $b^2(n_1-n_2)$ and $a^2(n_2-n_3)$, respectively, where n_i indicates the population in the level $|i\rangle$. The population difference in the ground-state sublevels is determined mainly by circular dichroism of the optical transitions from the ground state to the band, i.e., by the preferential depopulation with circularly polarized pump light. The values of n_i under the optical pumping are obtained from the steady-state solution of the rate equations. Only a small fraction of the pumped ions decays back to the ground state via the metastable state.[4] When the optical pumping time (~ 3 ms in our experiment) is much shorter than the spin-lattice-relaxation (SLR) time (order of a second[15]), and the complete nuclear spin memory in the repopulation to the ground-state sublevels[28] is assumed, we have $I_{12}:I_{23}=b^2u_+:a^2u_-$, where $u_\pm$ [$u_+:u_-\simeq 3:2$ for the σ^+ pumping or 2:3 for the σ^- pumping at 5800 Å, Fig. 5(a)] represents optical pumping rates from the $\pm$ electron-spin state. This ratio is consistent with the observed relative intensities both for the σ^+ and σ^- pumping ($a^2\simeq 0.7$, $b^2\simeq 0.3$ at ~ 100 Oe). If the randomized nuclear and electron spin return to the ground-state sublevels is assumed, we have $I_{12}:I_{23}=b^4u_+:a^4u_-$.

B. Signs of ESR signals and double pumping experiment

A remarkable experimental fact is that the metastable- and ground-state signals appear always in the opposite directions. When the sense of the circular polarization of the pump beam was inverted, all ESR signals were inverted, though the relative intensities of the signals were slightly changed because of the asymmetry of pumping effects for the σ^+ and σ^- lights. From this fact and the results of the double pumping experiment described below, we deduce the signs of the population differences responsible for the ground- and metastable-state signals.

We irradiated the sample with a linearly polarized light from the dye laser (5800 Å, 30 mW). No metastable-state signal was observed. However, an introduction of the second pumping with a circularly polarized σ^- light from another He-Ne laser (6328 Å, 50 mW) produced ESR signals as shown in Fig. 4. In contrast to the signals in Fig. 3, the metastable-state signals appear in the same direction as in the ground-state signals. For the σ^+ pumping all signals were inverted. The metastable-state signals disappeared when the pumping at 5800 Å was off. These features and the fact that the absorption coefficient for the transition from the ground state is small at 6328 Å, indicate that the metastable-state signals in Fig. 4 are due to the population differences created mainly by the preferential pumping from the metastable state.

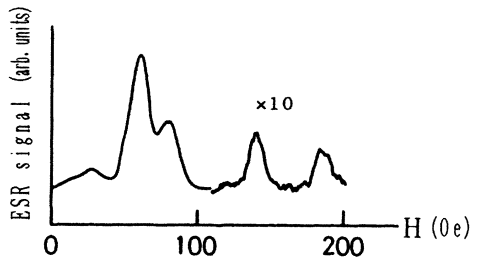

FIG. 4. ESR signals obtained from the double pumping experiment at the frequency 160 MHz under the pumping with linearly polarized (5800 Å, 30 mW) and circularly polarized (6328 Å, 50 mW) lights.

The absorption and MCD spectra for the ground state measured by Anderson and Sabisky[29] are shown in Figs. 5(a) and 5(b). The sign of the MCD for the metastable state can be inferred as follows. Since the ground and metastable states belong to the same irreducible representation $E_{5/2}$ of the point group O_h and electric-dipole transitions are allowed between the band and these states, the transitions from the ground and metastable states to the band should have essentially the same optical properties. Therefore, the sign of the MCD for the metastable state may be obtained from the MCD curve [Fig. 5(b)] for the ground state by shifting the origin of the energy (or wavelength) by an amount equal to the metastable-state energy [8928.6 cm^{-1} (Ref. 16)]. This procedure gives the same signs of the MCD's for the ground and metastable states. [The wavelength 6328 Å from the metastable state corresponds to 4043 Å in Fig. 5(b)]. This means that the MCD creates spin orientations in the same direction both in the ground and metastable states. Thus the population differences $n_1^*-n_2^*$, $n_2^*-n_3^*$, n_1-n_2, and n_2-n_3 responsible for the signals in Fig. 4 are of the same sign. It becomes clear that, when the changes of the magnetization are in the same direction in the ground and metastable states, we have signals of the same sign.

From this result and the comparison of the signals in Figs. 3 and 4, we conclude that the population differences n_1-n_2 and n_2-n_3 in the ground state and $n_1^*-n_2^*$ and $n_2^*-n_3^*$ in the metastable state for the signals in Fig. 3 are of opposite signs. In other words, when $n_1>n_2>n_3$ is achieved for the σ^+ pumping (or $n_1<n_2<n_3$ for the σ^- pumping) in the ground state, we have $n_1^*<n_2^*<n_3^*$ (or $n_1^*>n_2^*>n_3^*$) in the metastable state. We also observed that the (absolute value of) FR angle due to the optically induced magnetization in the ground state was decreased by the rf field. This indicates that the total mag-

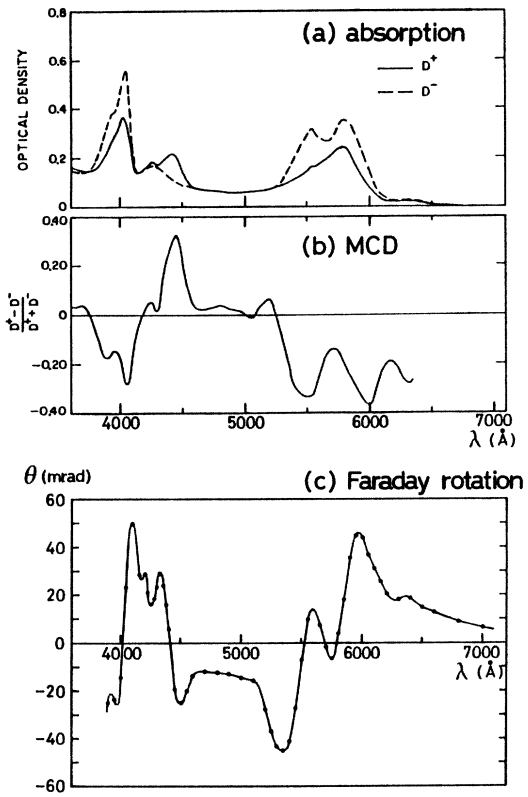

FIG. 5. (a) Absorption and (b) magnetic circular dichroism (MCD) spectra of Tm^{2+}:SrF_2 obtained by extrapolation to $\mu_B H/kT \rightarrow \infty$ (Ref. 27). D^+ in (a) refers to absorption for σ^+ light and D^- refers to σ^-. The fractional change is shown in (b). (c) Faraday rotation (FR) spectrum of Tm^{2+}:SrF_2 (0.02 at. % Tm^{2+}, 1 mm in thickness) obtained at 4.7 kOe and 1.9 K.

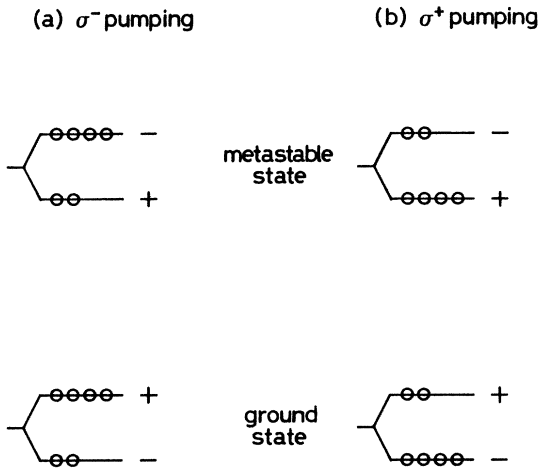

FIG. 6. Schematic spin polarization established in the ground and metastable states by the optical pumping and the spin memory.

netization in the ground state is along the direction determined by n_1, n_2, and n_3. We have no experimental data for the population n_4^*. However the theoretical considerations in paper III (Ref. 25) suggest that n_4^* is not so irregular as to upset the magnetization determined by n_1^*, n_2^*, and n_3^*. Thus we can say that the $\sigma^{\pm}$ pumping creates $\mp$ and $\pm$ magnetizations in the ground and metastable states, respectively.

The mechanism for establishing population difference in the metastable state is complicated. For the pumping at 5800 Å, the dominant mechanism is considered to be preferential pumping from the ground state to the band and the spin-orientation memory from the band to the metastable state. The SLR in the metastable state has little effect because the SLR time is longer than the lifetime of the metastable state.[13] The spin memory effect was extensively studied in Tm^{2+}:CaF_2 by Anderson and Sabisky[1] in high magnetic fields under an optical pumping with linearly polarized light incident perpendicular to the magnetic field. Our experiment is performed in low magnetic fields under an irradiation with circularly polarized light incident parallel to the magnetic field. In contrast to the case of Anderson and Sabisky the magnetization created in the metastable state is in the opposite direction to that in the ground state. Figure 6 schematically shows the spin orientations established in the ground and metastable states by the optical pumping and the spin memory, where $g^* < 0$ is taken into account. The spin memory effect will be discussed in detail in paper III. We will examine the spin memory in the transition from the $G_{3/2}$ states in the band to the metastable state assuming three possible symmetries of the decay, and show that the experimental results can be explained if the band has $J = \frac{7}{2}$, $G_{3/2}$ character and the decay has T_1 symmetry. The intensities of the metastable state signals (compared at the same magnetic field) in Fig. 3 are nearly equal. This shows that the population distribution in the metastable state is clearly different from that in the ground state. We will try to explain this point also in paper III.

The preferential pumping from the metastable state also affects the population distributions in that state. This effect will be described in Sec. IV D.

C. Measurement of Faraday rotation

The signs of the signals can also be analyzed by using the data of Faraday rotation (FR). We measured the FR spectrum between 4000 and 7000 Å at a high magnetic field (4.7 kOe) and a low temperature (1.9 K). In this situation FR was due to the thermalized ions in the ground state, and the contribution from the population in the metastable state was negligible. FR spectrum was measured in Tm^{2+}:CaF_2,[6] but no detailed measurement was made so far in Tm^{2+}:SrF_2.

We used a dc xenon arc as the light source. The radiation from the lamp, after passing through a monochromator, was collimated along the [111] axis, linearly polarized by a Glan prism, and focused on the sample (0.02 at. % Tm^{2+}, 1 mm in thickness) immersed in liquid helium (1.9 K). A static magnetic field was applied parallel to the [111] axis. The rotation angle of the polarization plane

was measured by a polarimeter. Figure 5(c) shows the observed FR spectrum. The spectral resolution is ~ 50 Å. The windows of the cryostat also show FR but this effect is subtracted in Fig. 5(c).

MCD and FR should be related through the Kramers-Kronig relationship. It is recognized that the FR spectrum [Fig. 5(c)] is nearly the dispersion of the MCD $(D^+ - D^-)$ obtained from Fig. 5(a).

The sign of the FR angle at 6328 Å (wavelength of the probe beam used in the ESR experiment) is positive. It shows that if we apply an rf field when $n_1 > n_2 > n_3$, the FR angle is decreased.

The shape of the FR spectrum for the metastable state can be inferred by using an argument similar to that used for MCD in Sec. IV B, i.e., by shifting the origin of the energy (or wavelength) of Fig. 5(c) by an amount equal to the metastable-state energy. The sign of the FR angle at 6328 Å due to the metastable state is the same (positive) with that at 4043 Å in Fig. 5(c). Therefore the metastable-state ESR, when $n_1^* > n_2^* > n_3^*$, results in a decrease of the FR angle. These results lead to the same conclusion about the population distributions as Sec. IV B.

D. Effect of preferential pumping from the metastable state

The effect of preferential pumping from the metastable state has been demonstrated in the double pumping experiment. This effect exists even in the single pumping experiment where the population distributions in the metastable state are mainly determined by the preferential pumping from the ground state followed by the spin orientation memory.

We observed ESR signals by changing the wavelength of the pumping light from 5750 to 5950 Å (Fig. 7). The metastable-state signals became smaller as the wavelength became longer. The lower-field line of the metastable-state signals disappeared at 5900 Å and then reappeared in the opposite direction at 5950 Å, or in the same direction as the ground-state signals. These can be explained as an effect of preferential pumping from the metastable state.

As described in Sec. IV B, the sign of the MCD of the transition from the metastable state is the same as that of the ground state between 5750 and 5950 Å. [The wavelengths 5750 and 5950 Å from the metastable state correspond to 3799 and 3885 Å in Fig. 5(b)]. The preferential pumping from the metastable state tends to create spin orientations in the same direction both in the ground and metastable states, whereas the preferential pumping from the ground state followed by the spin memory creates spin orientations in the opposite directions in the ground and metastable states. The results in Fig. 7 can be understood as the competition of these effects. As the wavelength becomes longer, the effect of preferential pumping (MCD and absorption coefficient) from the metastable state becomes larger. At 5800 Å, where most of our experiments were made, the contribution of the spin memory is dominant. The dispersion shape of the higher-field line at 5950 Å is due to the magnetic cross relaxations discussed in the next section.

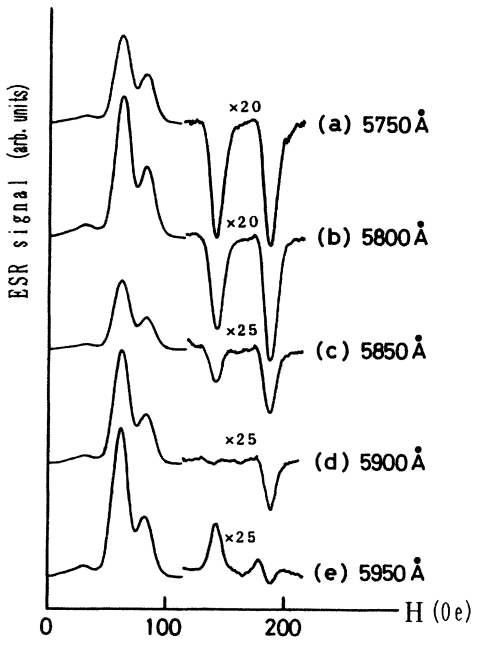

FIG. 7. Dependence of the ESR signals on the wavelength of the pumping light (σ^-, 30 mW) at the frequency 160 MHz. For the ground-state signals the amplifier gain in (c)—(e) is 2.5 times smaller than that in (a) and (b).

V. CROSS RELAXATION

A. Anomalous behavior of the ESR signal

We found that the ESR signals in the metastable state exhibited anomalous behavior as shown in Fig. 8 when the frequency of the rf field was varied between 135 and 155 MHz. At 135 MHz two downward (negative) signals similar to those in Fig. 3 are observed. As the frequency is increased the higher-field line (1*-2* line) changes its shape in a complicated manner and becomes positive at 145 MHz (at $H = 167$ Oe), while the lower-field line (2*-3* line) remains unchanged except for the shift. Figure 9(a) shows the dependence of the signals at 145 MHz on the pumping power of the laser. As the power is increased the signal at 167 Oe grows and after passing through the maximum it becomes smaller. Figure 9(b) shows the dependence of the signals at 145 MHz on the chopping frequency of the rf field. As the frequency is increased both lines become small. The higher-field line decreases more rapidly than the lower-field line, indicating that the time response of the higher-field line to the rf field is slower than that of the lower-field line.

In order to examine the behavior more directly, we observed the time dependence of the ESR signal. A rf field (150 MHz) was applied for 10 msec at a repetition frequency of 20 Hz and the output of the polarimeter was amplified and then accumulated by an averager. Figure 10 shows the time evolution of the polarimeter output. The three magnetic fields in Fig. 10 correspond to the maximum (167 Oe), the center (172 Oe), and the minimum (177 Oe) of the higher-field line at 150 MHz in

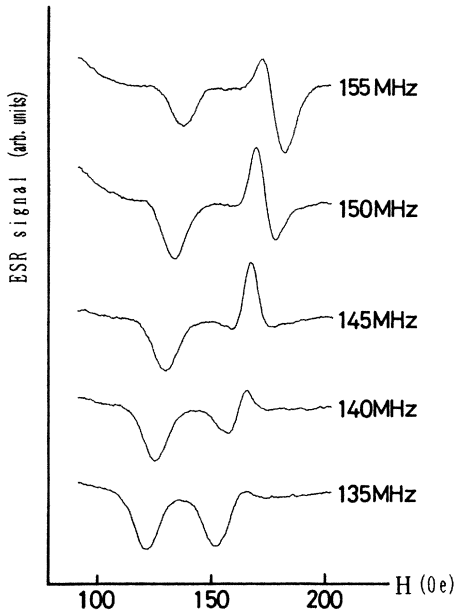

FIG. 8. Frequency dependence of the metastable-state ESR signals between 135 and 155 MHz under the pumping with σ^- light (5800 Å, 15 mW).

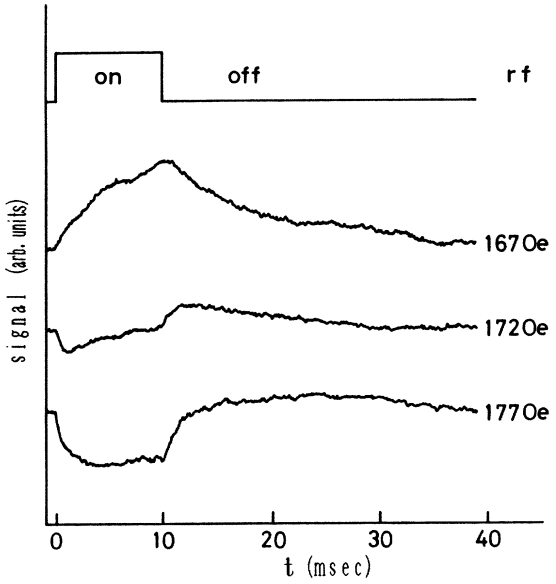

FIG. 10. Time dependence of the metastable-state ESR signal (the higher-field line) at the frequency 150 MHz with circularly polarized light (5800 Å, 15 mW). The rf field is applied for 10 msec and the rf pulses are repeated at 20 Hz. The three magnetic fields correspond to the maximum (167 Oe), the center (172 Oe), and the minimum (177 Oe) of the higher-field line at 150 MHz in Fig. 8.

Fig. 8. At 177 Oe the polarimeter output decreases while the rf field is on and then recovers. This can be regarded as a normal time dependence of the ESR signal, since similar dependence was observed for the lower-field line; the population difference is destroyed by the rf field and then created by the optical pumping. At 167 Oe, on the other hand, the output shows anomalous behavior; the direction of the change is opposite, and the time constants are longer than those at 177 Oe. The behavior at 172 Oe is a mixture of those at 177 and 167 Oe.

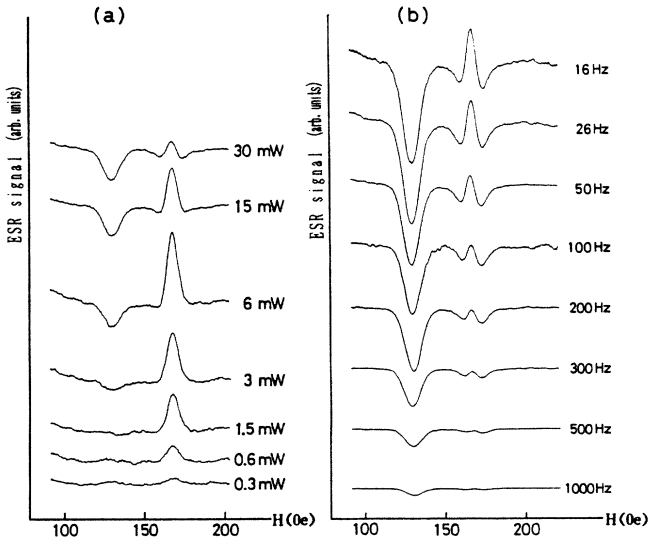

FIG. 9. Dependences of the metastable-state ESR signals (a) on the pumping power of the laser and (b) on the chopping frequency of the rf field at 145 MHz under the pumping with σ^- light at 5800 Å. The chopping frequency in (a) is 26 Hz and the pumping power in (b) is 20 mW.

B. Explanation of the anomalous behavior

In this section we will give a qualitative explanation of the anomalous behavior as an effect of the metastable-state—ground-state cross relaxation enhanced by the ground-state—ground-state cross relaxation. Calculations show that the frequency of the transition 1*-4* in the metastable state coincides with that of 2-4 in the ground state at 161.2 Oe (Fig. 1). If the cross relaxation [metastable-state—ground-state (MS-GS) cross relaxation] occurs at this field, the populations in the levels 1* and 4* are changed, while the populations in the other levels in the metastable state are unchanged. Therefore it is expected that the anomalous behavior which is observed only for the higher-field line (1*-2* line) is related to this MS-GS cross relaxation.

However, the explanation is not straightforward. We have to explain why the positive peak appears at 167 Oe which deviates from the expected cross relaxation field of 161.2 Oe. Our explanation is as follows. Calculation also shows that another cross relaxation (GS-GS cross relaxation) in the ground state is expected to occur at 171.5 Oe where the frequencies of the transitions 1-3 and 3-4 become equal (Fig. 1). The crossing fields for the MS-GS and GS-GS cross relaxations are separated by ~ 10 Oe.

However, the linewidths of the cross relaxations are considered to be comparable to the separation, the MS-GS and GS-GS cross relaxations may occur simultaneously, most frequently in the middle of the crossing fields ($\sim$167 Oe). We consider the case of σ^- pumping as in Fig. 8, where $n_1 < n_2 < n_3$ and $n_1^* > n_2^* > n_3^*$ are achieved, and the net magnetization is positive in the ground state and negative in the metastable state. From a brief inspection of the optical pumping process, we can safely assume, in the following, that polarizations ($|n_i^* - n_j^*| / |n_i^* + n_j^*|$) in the metastable state are smaller than those in the ground state, and that n_3 is larger than n_4. If the GS-GS cross relaxation occurs, the population difference $n_4 - n_2$ is increased because n_4 is increased leaving n_2 unchanged. Therefore, n_i^* is increased as a result of the MS-GS cross relaxation. This means that $n_1^* - n_2^*$ becomes larger at 167 Oe, and a negative enhanced signal is expected at this field. However, the observed signal is positive in contradiction to the prediction.

The apparent discrepancy can be resolved as follows. Our optical detection scheme detects the changes of population differences both in the ground and metastable states. The rf field decreases the population difference $n_1^* - n_2^*$ and therefore also decreases $n_1^* - n_4^*$ in the metastable state. At the crossing point, this accompanies the decrease of the population difference $n_4 - n_2$ in the ground state through the MS-GS cross relaxation. This also decreases n_3 and increases n_1 through the GS-GS cross relaxation, i.e., decreases the magnetization in the ground state. The observed signal represents the sum of the contributions from the ground and metastable states. If the contribution from the ground state is dominant, the ESR signal may be positive. Since $|1\rangle$ and $|3\rangle$ are $|--\rangle$ and $|++\rangle$ states, it is expected that the decrease of n_3 and the increase of n_1 results in the decrease of the magnetization in the ground state and gives a strong positive signal which overcomes the negative signal due to the decrease of $n_1^* - n_2^*$ or the increase of the magnetization in the metastable state.

A signal of similar nature was also observed at about 220 Oe in the middle of the crossing fields 205.5 Oe ($E_{34}^* = E_{13}$) and 228.7 Oe ($E_{23} = E_{34}$). But the anomaly of the signal was small because the separation of the crossing fields is large.

At the MS-GS crossing field 161.2 Oe, the effect of GS-GS cross relaxation is not significant. Therefore no efficient population redistribution or change of magnetization in the ground state accompanied by the metastable-state ESR is expected. Actually, the effect due only to the MS-GS cross relaxation was recognized in Fig. 8 as a small decrease of the signal intensity of the higher-field line at 135 MHz near the crossing field (161.2 Oe). The intensity of the higher-field line is usually stronger than the lower-field line as in Fig. 3.

The pumping-power dependence in Fig. 9(a) can be explained by the change of the population in the ground state, and supports the above model for the positive signal at 167 Oe. When the power is too strong the higher-field line becomes small. This can be understood as a result of the competition between the optical pumping time and the MS-GS cross relaxation time. The effect of the cross relaxation which gives the positive signal is decreased when the pumping time becomes shorter than the cross relaxation time.

The ESR line is inhomogeneously broadened and the rf field directly excites a narrow part of the line. However, the spectral diffusion is fast enough to transfer the excitation over the whole line before the cross relaxations take place. The spectral-diffusion time measured by the stimulated-spin-echo experiment[3] is 3 μsec/4.5 MHz ($\tau_{12} = 220$ nsec) in 0.0026 at. % Tm^{2+}:CaF_2.

Generally, there are three types of metastable-state signals: (1) pure (negative) ESR signal due only to the population change in the metastable state, (2) ESR signal affected by the MS-GS cross relaxation whose intensity is reduced by the population change in the ground state, and (3) positive ESR signal due to the effect of the MS-GS cross relaxation enhanced by the GS-GS cross relaxation. When the frequency of the rf field, or the resonance field for the transition (1*-2*) is far from the crossing field, only pure ESR signals are observed. When the resonance field is near the MS-GS crossing field, the signal of type (2) is observed. The signal of type (3) has a peak in the middle of the MS-GS and GS-GS crossing fields. Generally a superposition of these types of signals is observed. If we use an optical detection scheme sensitive only to the magnetization change in the metastable state, for instance, probing with infrared light, the observed pattern of the signal should be different.

According to the model described above, the growth and decay times of the signal at 167 Oe in Fig. 10 are related to the GS-GS and MS-GS cross-relaxation times. In addition, optical and rf pumping times and the lifetime of the metastable state must be taken into account. We measured the ground-state cross-relaxation times by another experiment using a pulse pumping with a nitrogen-laser-pumped dye laser. The details are planned to be published later. The cross-relaxation time at 171.5 Oe ($E_{13} = E_{34}$) was $\sim$2 msec. The observed time constants are much longer than this cross-relaxation time and the optical and rf pumping times. Therefore it is considered that the growth and decay times are mainly determined by the MS-GS cross relaxation time and the lifetime of the metastable state. The observed time constants are all comparable to the lifetime of the metastable state, whose value of 13 msec was obtained from the fluorescence. Therefore the MS-GS cross relaxation time should not be significantly different from the lifetime of the metastable state. Since the magnetic-dipole transition is forbidden for the transition 2-4, such a long time constant is reasonable.

The chopping-frequency dependence in Fig. 9(b) is explained by the difference of the time response. The time response of the lower-field line is determined by the rf pumping time and the optical pumping time, while that of the higher-field line is determined by the MS-GS cross-relaxation time and the lifetime of the metastable state.

[1]C. H. Anderson and E. S. Sabisky, Phys. Rev. **178**, 547 (1969).
[2]L. F. Mollenauer, W. B. Grant, and C. D. Jeffries, Phys. Rev. Lett. **20**, 488 (1968).
[3]E. S. Sabisky and C. H. Anderson, Appl. Phys. Lett. **13**, 214 (1968).
[4]Z. J. Kiss, Phys. Rev. **127**, 718 (1962).
[5]R. C. Duncan, Jr. and Z. J. Kiss, Appl. Phys. Lett. **3**, 23 (1963).
[6]Y. R. Shen, Phys. Rev. **134**, A661 (1964).
[7]H. A. Weakliem and Z. J. Kiss, J. Chem. Phys. **41**, 1507 (1964).
[8]B. P. Zakharchenya, V. P. Makarov, A. V. Varfolomeyev, and A. Ya. Ryskin, Opt. Spektrosk. **16**, 455 (1964) [Opt. Spectrosc. (USSR) **16**, 248 (1964)].
[9]C. H. Anderson, H. A. Weakliem, and E. S. Sabisky, Phys. Rev. **143**, 223 (1966).
[10]C. Pedrini, D. S. McClure, and C. H. Anderson, J. Chem. Phys. **70**, 4959 (1979).
[11]W. Hayes and J. W. Twidell, J. Chem. Phys. **35**, 1521 (1961).
[12]R. G. Bessent and W. Hayes, Proc. R. Soc. London, Ser. A **285**, 430 (1965).
[13]E. S. Sabisky and C. H. Anderson, Phys. Rev. **148**, 194 (1966).
[14]E. S. Sabisky and C. H. Anderson, IEEE J. Quantum. Electron. **QE-3**, 287 (1967).
[15]E. S. Sabisky and C. H. Anderson, Phys. Rev. B **1**, 2028 (1970).
[16]W. Hayes and P. H. S. Smith, J. Phys. C **4**, 840 (1971).
[17]E. B. Aleksandrov and V. S. Zapasskii, Fiz. Tverd. Tela (Leningrad) **19**, 3083 (1977) [Sov. Phys.—Solid State **19**, 1802 (1977)].
[18]E. B. Aleksandrov and V. S. Zapasskii, Fiz. Tverd. Tela (Leningrad) **20**, 1180 (1978) [Sov. Phys.—Solid State **20**, 679 (1978)].
[19]A. L. Konkin, V. P. Meiklyar, and M. L. Falin, Opt. Spektrosk. **51**, 946 (1981) [Opt. Spectrosc. (USSR) **51**, 525 (1981)].
[20]G. Strauch, Th. Vetter, and A. Winnacker, Phys. Lett. **94A**, 160 (1983).
[21]H. A. Weakliem, C. H. Anderson, and E. S. Sabisky, Phys. Rev. B **2**, 4354 (1970).
[22]C. H. Anderson and E. S. Sabisky, in *Physical Acoustics,* edited by W. P. Mason and R. N. Thurston (Academic, New York, 1971), Vol. VIII, p. 19.
[23]T. Kohmoto, Y. Fukuda, M. Tanigawa, T. Mishina, and T. Hashi, Phys. Rev. B **28**, 2869 (1983).
[24]T. Kohmoto, Y. Fukuda, and T. Hashi, following paper, Phys. Rev. B **34**, 6094 (1986).
[25]T. Kohmoto, Y. Fukuda, and T. Hashi (unpublished).
[26]R. V. Jones, Proc. R. Soc. London, Ser. A **349**, 423 (1976).
[27]E. B. Alexandrov and V. S. Zapasskii, Opt. Spektrosk. **41**, 855 (1976) [Opt. Spectrosc. (USSR) **41**, 502 (1976)].
[28]W. B. Grant, L. F. Mollenauer, and C. D. Jeffries, Phys. Rev. B **4**, 1428 (1971).
[29]C. H. Anderson and E. S. Sabisky, in *Physical Acoustics,* Ref. 22, p. 21.
[30]M. Mitsunaga, Ph.D. thesis, University of California, Berkeley, 1983.